Electronic Supplementary Material (ESI) for Physical Chemistry Chemical Physics.

ELECTRONIC SUPPLEMENTARY INFORMATION - ESI

Solvent Effect on the Excited-State Double Proton Transfer Mechanism in 7-Azaindole Dimer: A TDDFT Study with Polarizable Continuum Model

Xue-fang Yu, Shohei Yamazaki, Tetsuya Taketsugu

Table S1. PCM parameters in all solvents.

solvent	hexane	heptane	cyclohexane	benzene	diethyl ether	chloroform	dichloromethane	methanol	acetonitrile	water
static dielectric constant	1.88	1.92	2.02	2.25	4.34	4.90	8.93	32.63	36.64	78.39
optical analog	1.918	1.918	2.028	2.24	1.830	2.085	2.028	1.758	1.806	1.776
solvent radius	3.74	3.12	2.82	2.63	3.46	2.48	2.94	1.86	2.15	1.385

Table S2. Electronic energy for the highest point in the concerted and stepwise reaction paths in LE state, relative to ND_{LE} (in kcal/mol) under non-equilibrium solvent effect.

solvent	heptane	cyclohexane	benzene	diethyl ether	chloroform	dichloromethane	methanol	acetonitrile	water
static dielectric constant	1.92	2.02	2.25	4.34	4.90	8.93	32.63	36.64	78.39
TS_{LE}	6.79	6.81	6.83						
TS_{LE1}				6.80	6.83	6.83	6.86	6.86	6.87
TS_{LE2}				4.74	4.79	4.85	4.88	4.89	4.90

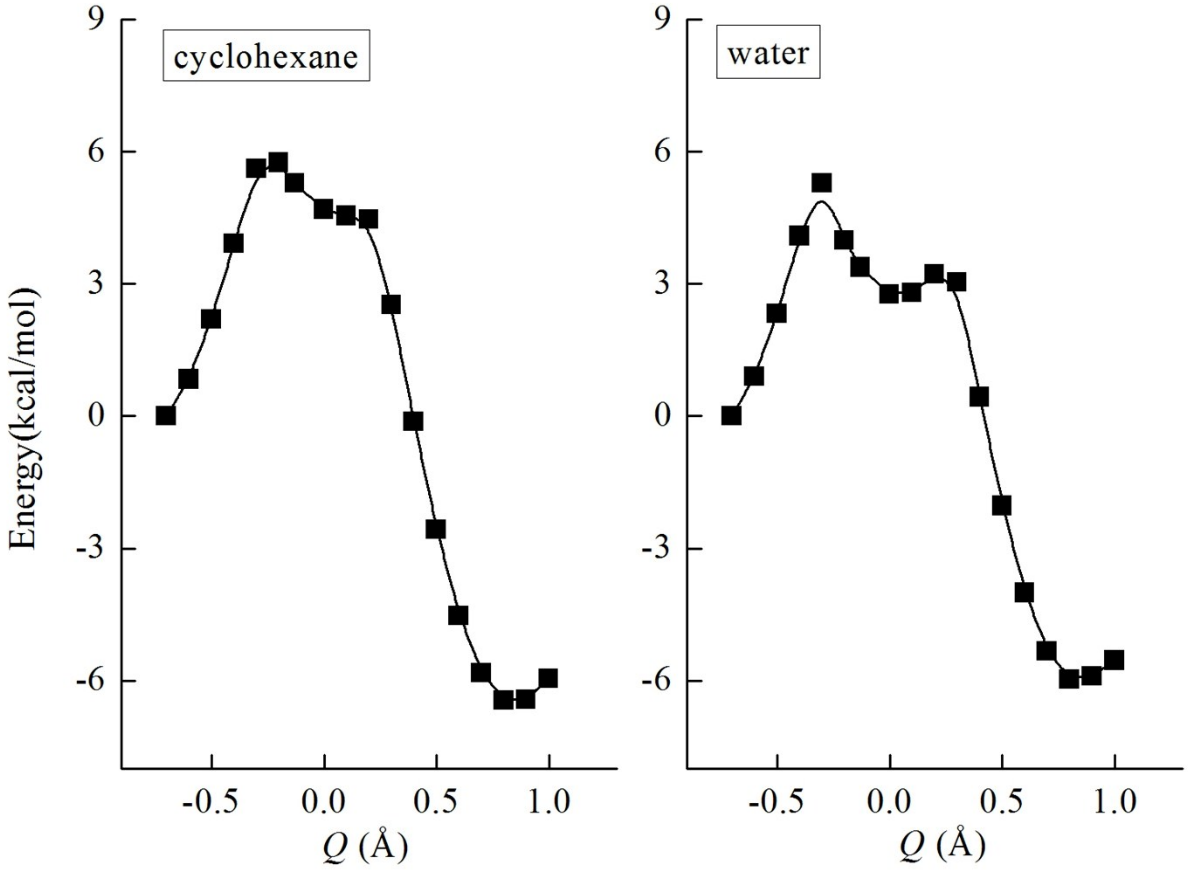

Figure S1. Potential energy profile along MEP in LE state as a function of the reaction coordinate *Q* in cyclohexane and water at the TD-CAM-B3LYP/6-31+G* level.

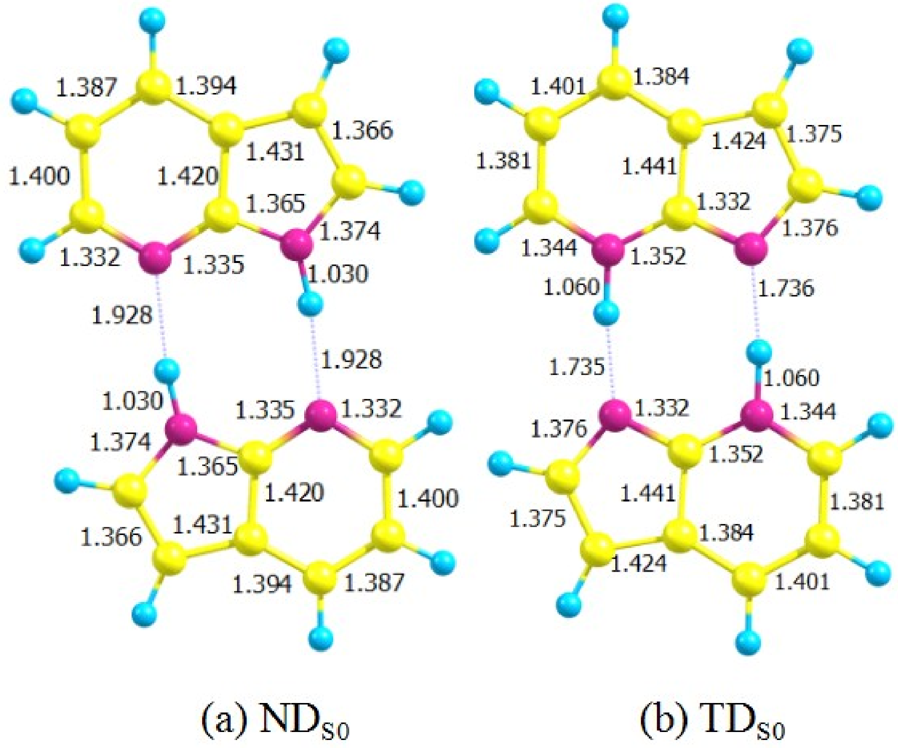

(a) ND_{S0} (b) TD_{S0}

Figure S2. Equilibrium geometries of 7AI dimer in the S_0 state: (a) ND_{S0} and (b) TD_{S0} optimized at the CAM-B3LYP level in the gas phase.

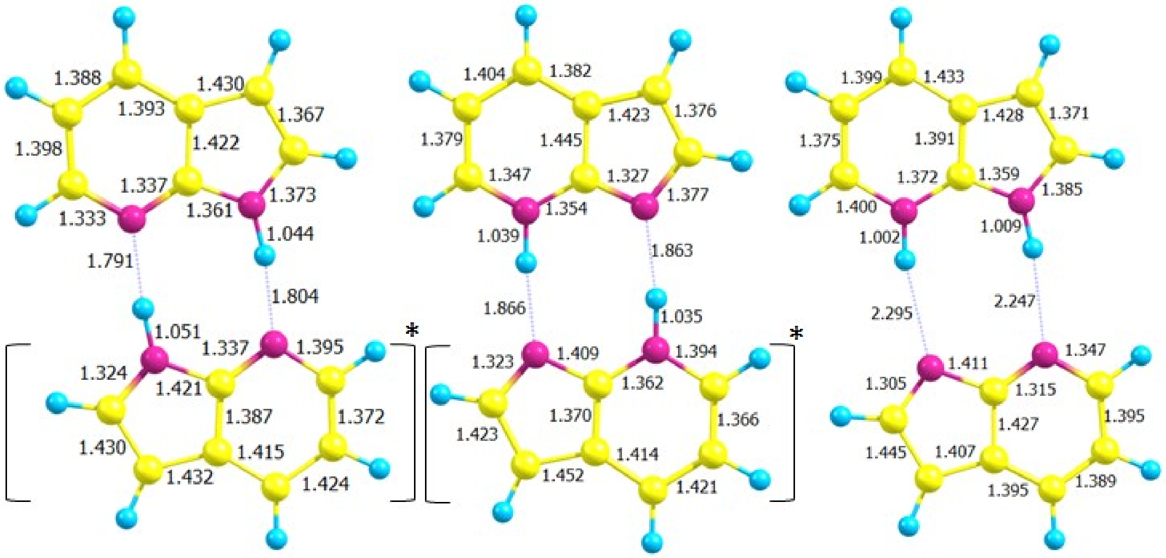

(a) $\mathrm{ND_{LE}}$ (b) $\mathrm{TD_{LE}}$ (c) $\mathrm{INT_{CT}}$

Figure S3. Equilibrium geometries of 7AI dimer in the S_1 state, optimized at the TD-CAM-B3LYP level: (a) $\mathrm{ND_{LE}}$, (b) $\mathrm{TD_{LE}}$ and (c) $\mathrm{INT_{CT}}$ in the gas phase.

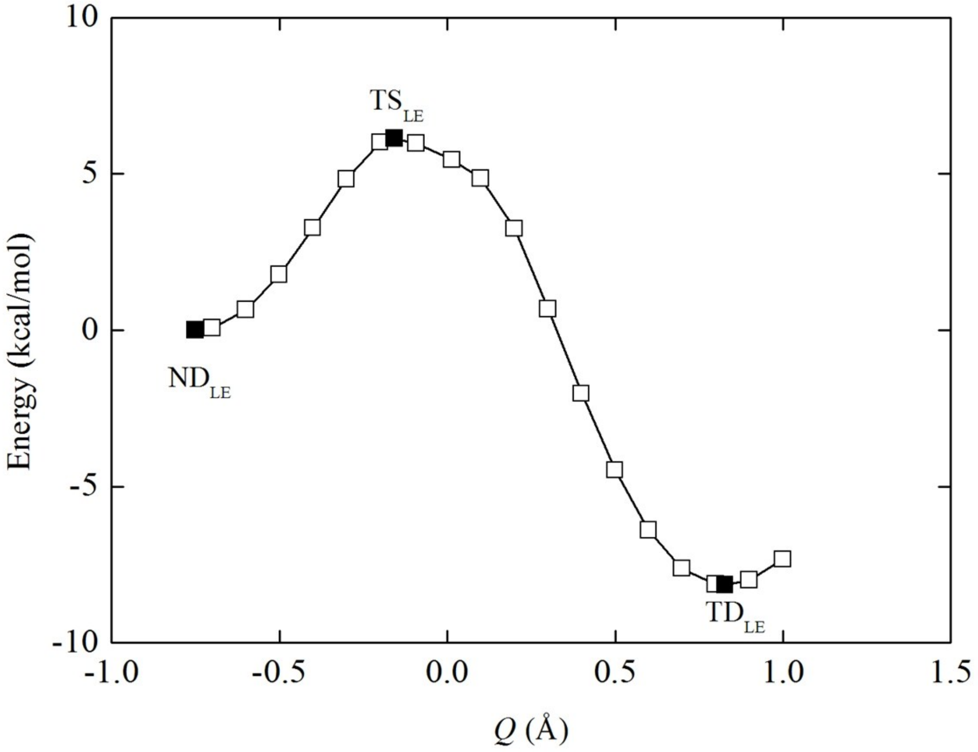

Figure S4. Potential energy profile along MEP in LE state as a function of the reaction coordinate Q in the gas phase at the TD-CAM-B3LYP level.

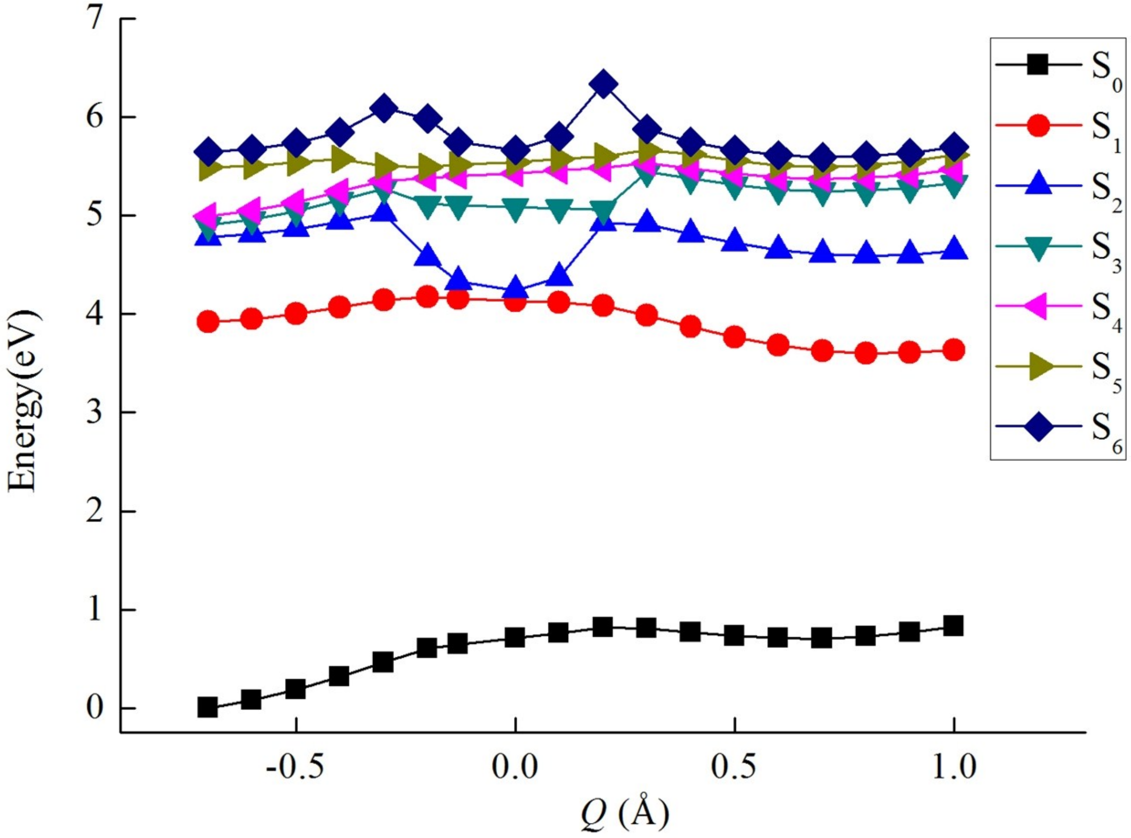

Figure S5a. Potential energy curves of the lowest 6 excited states along cMEPs as a function of the reaction coordinate *Q* in non-polar solvent heptane.

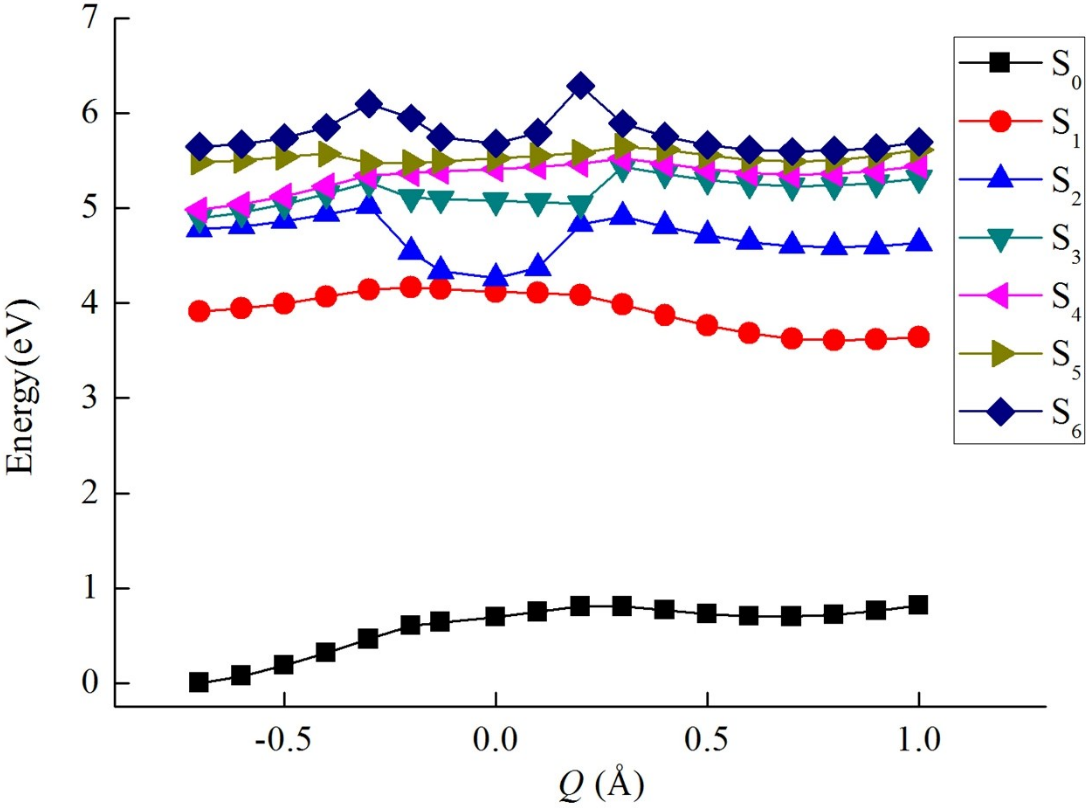

Figure S5b. Potential energy curves of the lowest 6 excited states along cMEPs as a function of the reaction coordinate *Q* in non-polar solvent benzene.

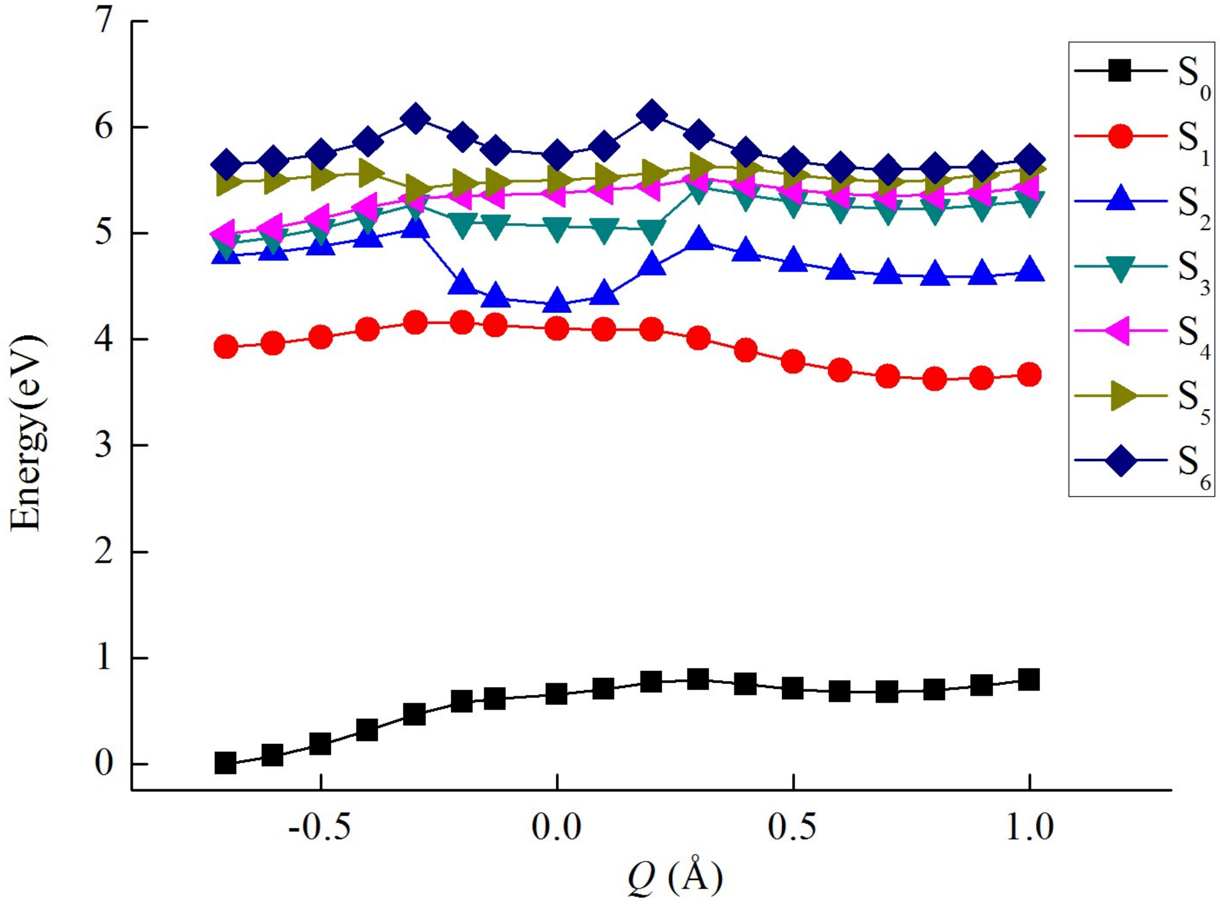

Figure S5c. Potential energy curves of the lowest 6 excited states along cMEPs as a function of the reaction coordinate *Q* in polar solvent diethyl ether.

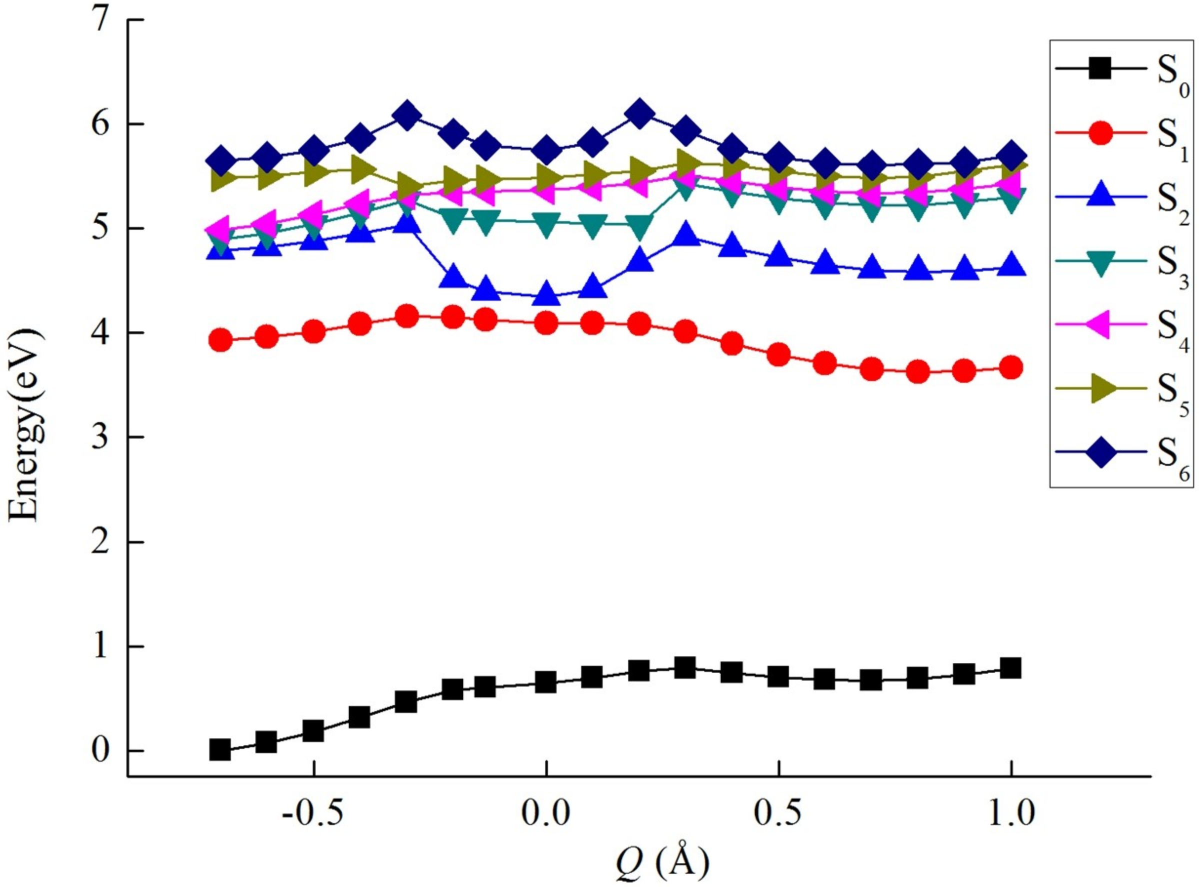

Figure S5d. Potential energy curves of the lowest 6 excited states along cMEPs as a function of the reaction coordinate Q in polar solvent chloroform.

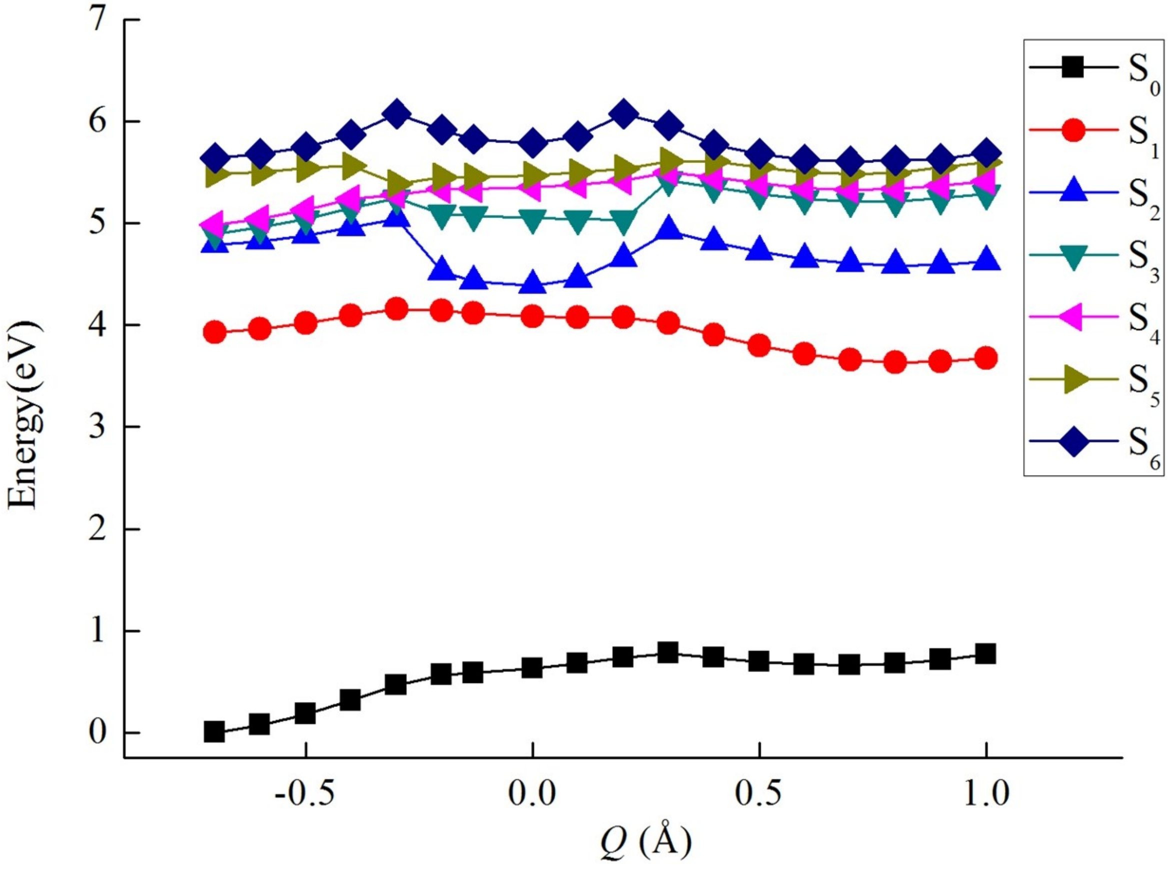

Figure S5e. Potential energy curves of the lowest 6 excited states along cMEPs as a function of the reaction coordinate *Q* in polar solvent dichloromethane.

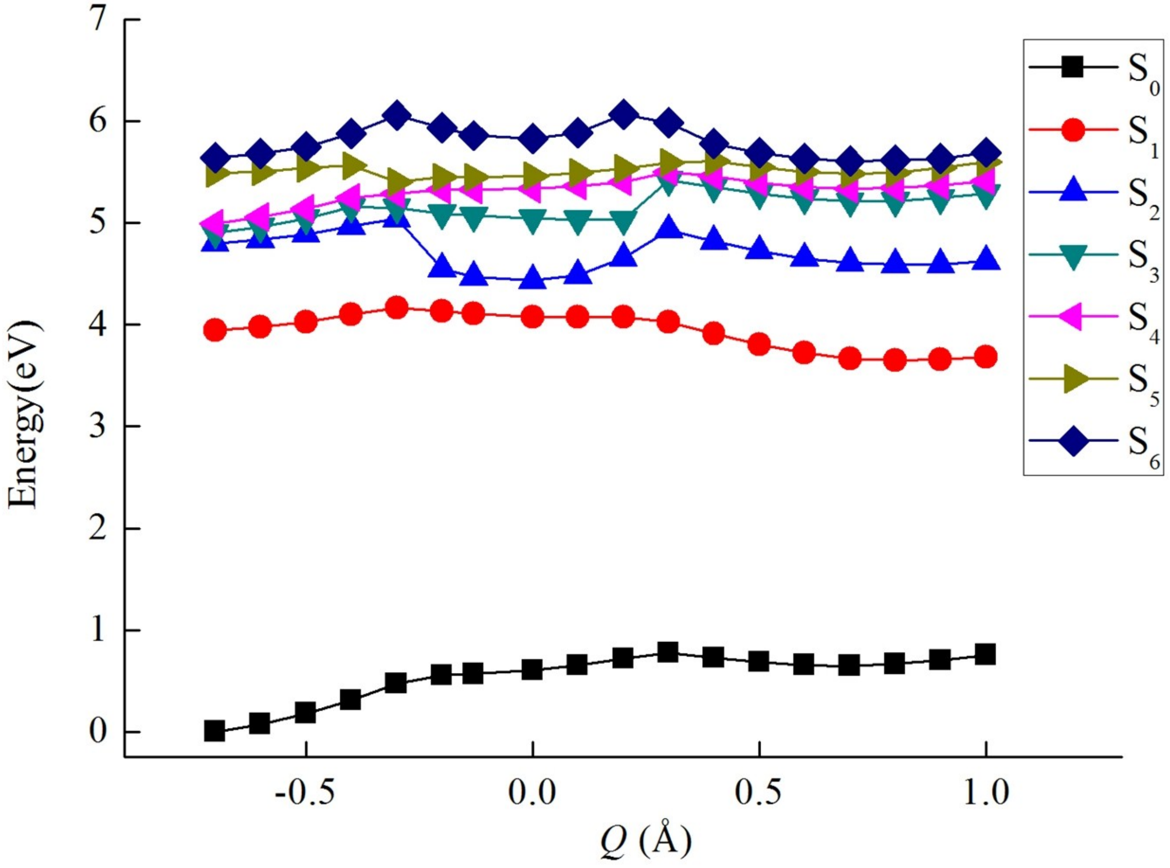

Figure S5f. Potential energy curves of the lowest 6 excited states along cMEPs as a function of the reaction coordinate Q in polar solvent methanol.

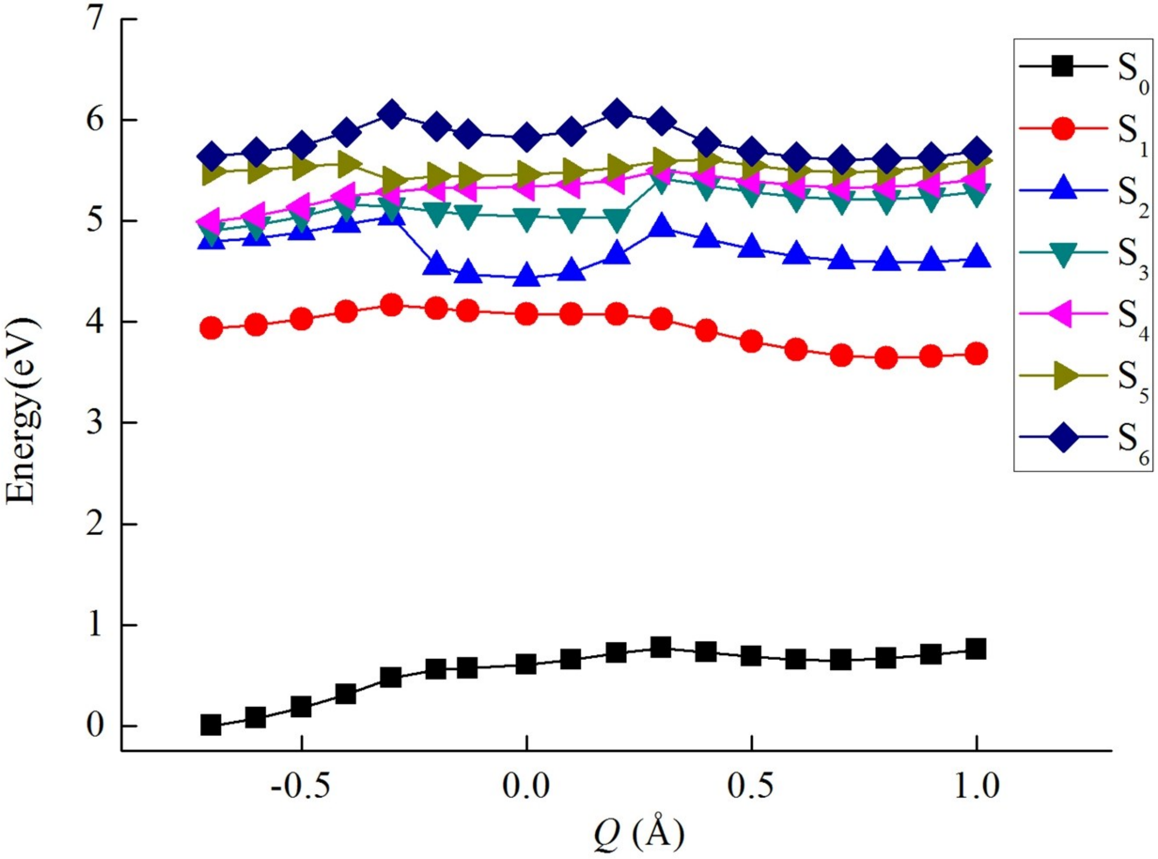

Figure S5g. Potential energy curves of the lowest 6 excited states along cMEPs as a function of the reaction coordinate *Q* in polar solvent acetonitrile.

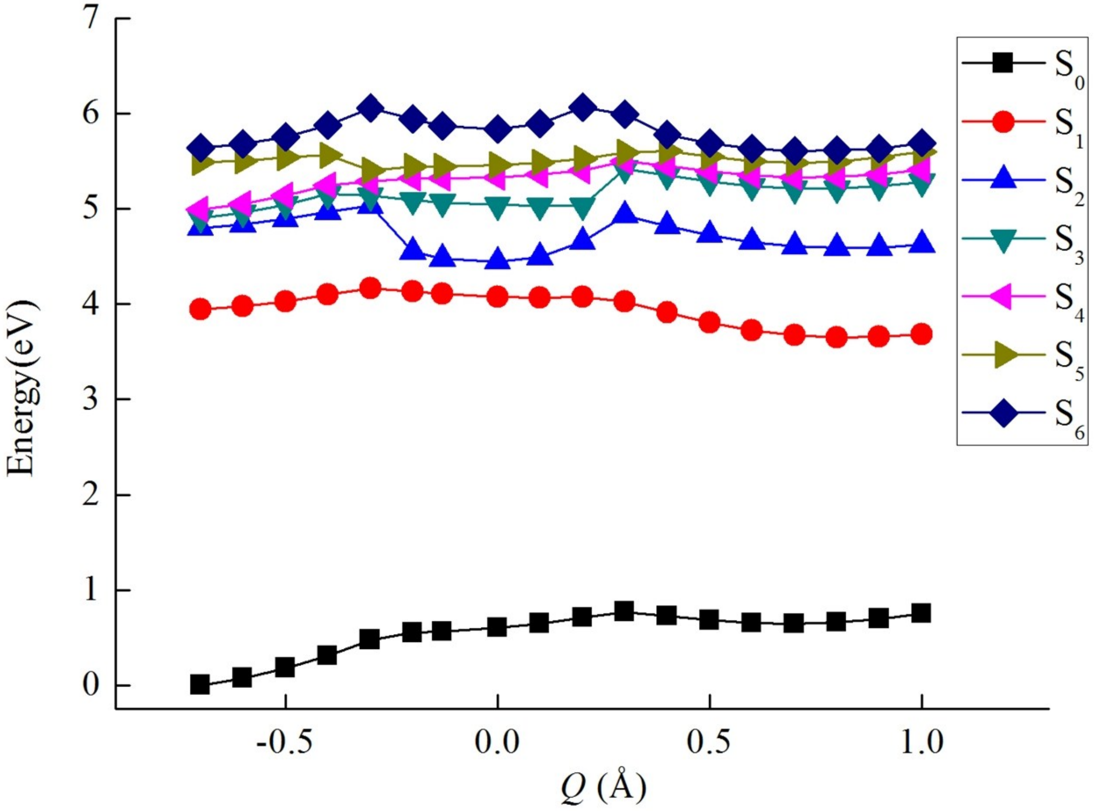

Figure S5h. Potential energy curves of the lowest 6 excited states along cMEPs as a function of the reaction coordinate *Q* in polar solvent water.

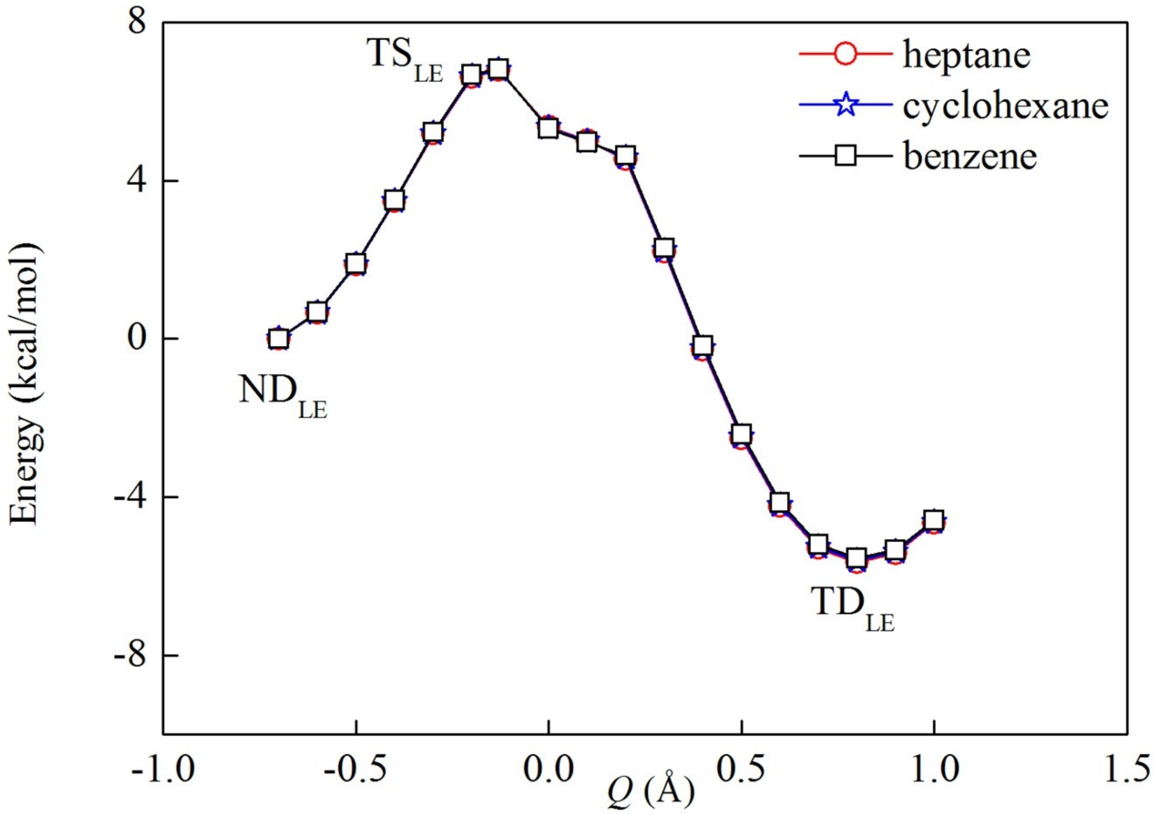

Figure S6. Potential energy curves along cMEPs in LE state as a function of the reaction coordinate *Q* in non-polar solvents heptane, cyclohexane and benzene considering the non-equilibrium solvent effect..

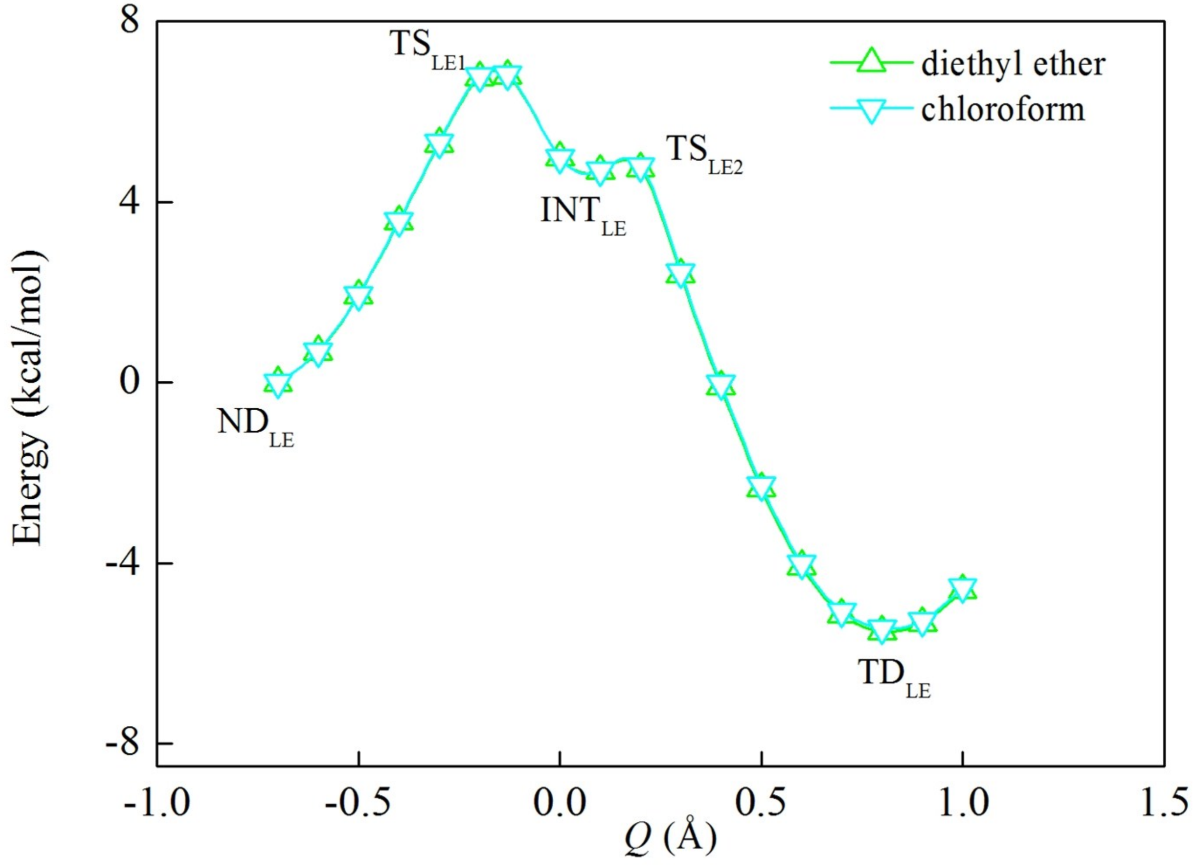

Figure S7a. Potential energy curves along cMEPs in LE state as a function of the reaction coordinate *Q* in polar solvents diethyl ether, and chloroform considering the non-equilibrium solvent effect.

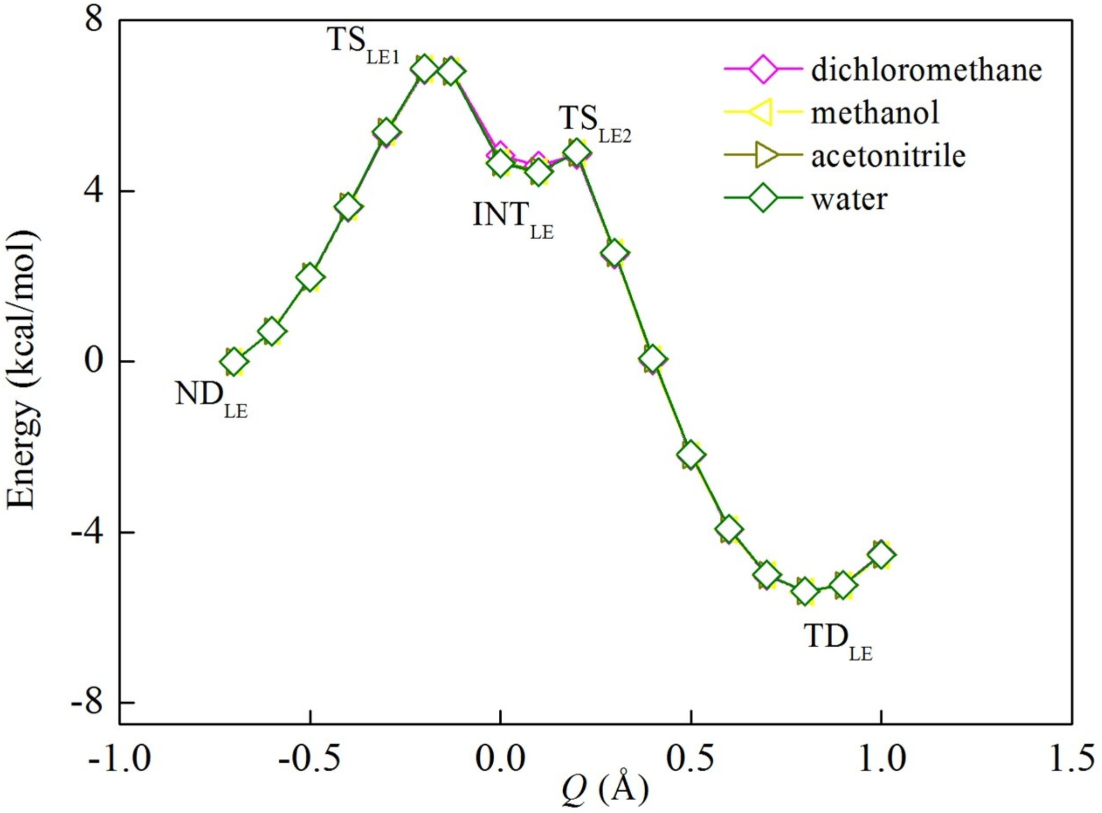

Figure S7b. Potential energy curves along cMEPs in LE state as a function of the reaction coordinate *Q* in polar solvents dichloromethane, methanol, acetonitrile and water considering the non-equilibrium solvent effect.

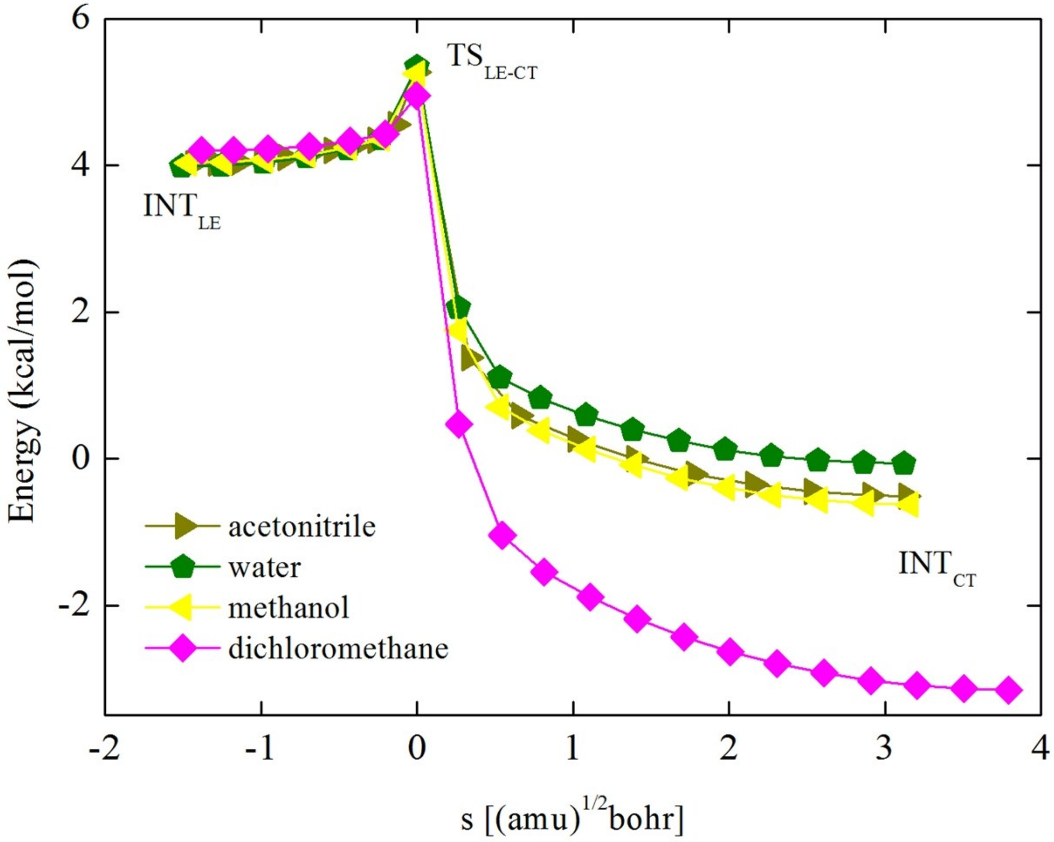

Figure S8. Potential energy profiles along IRC paths from INT_{CT} to INT_{LE} in polar solvents at TD-CAM-B3LYP/PCM level.